Forensic Chemistry 29 (2022) 100421

Contents lists available at ScienceDirect

Forensic Chemistry

journal homepage: www.sciencedirect.com/journal/forensic-chemistry

Combining FTIR-ATR and OPLS-DA methods for magic mushrooms discrimination

Cátia S.M. Esteves [a,*], Elena M.M. de Redrojo [c], José Luis García Manjón [b], Gabriel Moreno [b], Filipe E. Antunes [a], Gemma Montalvo [c,e], Fernando E. Ortega-Ojeda [c,d,e,*]

[a] CQC, Department of Chemistry, University of Coimbra, Rua Larga, 3004-535 Coimbra, Portugal
[b] Universidad de Alcalá, Departamento de Ciencias de la Vida, Ctra. Madrid-Barcelona km 33.6, Alcalá de Henares, Madrid 28864, Spain
[c] Universidad de Alcalá, Departamento de Química Analítica, Química Física e Ingeniería Química, Ctra. Madrid-Barcelona km 33.6, Alcalá de Henares, Madrid 28864, Spain
[d] Universidad de Alcalá, Departamento de Ciencias de la Computación, Ctra. Madrid-Barcelona km 33.6, Alcalá de Henares, Madrid 28864, Spain
[e] Universidad de Alcalá, Instituto Universitario de Investigación en Ciencias Policiales, Libreros 27, Alcalá de Henares, Madrid 28801, Spain

ARTICLE INFO

Keywords:
Hallucinogenic mushrooms
FTIR-ATR
OPLS-DA
Drugs

ABSTRACT

Magic mushrooms are naturally occurring fungi that are considered hallucinogenic drugs because they contain psilocybin and psilocin. These substances are controlled in almost every country in the world, so the use, possession, cultivation, and sale of magic mushrooms are prohibited in whole or in part. Despite this, the abuse of magic mushrooms continues and can put at risk the life of the consumer and society in general if the consumer behaves in an unsafe manner.

The number of mushroom species is very high, making it difficult to correctly identify them based only on physical and morphological characteristics. Therefore, there is a need to develop non-destructive mushrooms analysis methods that have less response time and higher discrimination ability. The present work used Attenuated Total Reflectance Fourier Transform Infrared (FTIR-ATR) Spectroscopy to study 64 mushroom samples from different genera including hallucinogenic, edible, and toxic species. In addition, this study used Orthogonal Partial Least Squares - Discriminant Analysis (OPLS-DA), using SIMCA chemometric software to analyse the obtained infrared (IR) spectra. The main molecular vibrations of the components of the fungus were successfully identified by IR spectroscopy. Although the specific bands corresponding to psilocybin or psilocin could not be assigned in the spectra, the regression method was able to discriminate the various species. Hallucinogenic mushrooms were well separated from other species, allowing the method to be used as an initial screening technique to determine whether or not the seized mushrooms are of forensic interest.

1. Introduction

Hallucinogenic mushrooms, "shrooms" or "magic mushrooms" as they are commonly called, are fungi that naturally synthesize molecules with hallucinogenic properties. These properties are due to specific compounds, such as psilocybin ([3-[2-(dimethylamino)ethyl]-1H-indol-4-yl] Dihydrogen phosphate) and psilocin (3-[2-(dimethylamino)ethyl]-1H-indol-4-ol), which are the most commonly found compounds in hallucinogenic species [1–3]. Their indolealkylamine structure is associated with hallucinogenic activity. Due to their mechanism of action and corresponding effects, magic mushrooms belong to the group of hallucinogenic or psychedelic drugs.

Ancient civilizations used magic mushrooms as medicine or for religious purposes. Nonetheless, the abuse of hallucinogenic mushrooms as a recreational activity is more recent. In fact, available data report such abuse since the 1960 s decade [4,5]. Psilocybin and psilocin were added to the United Nations Convention's Schedule I of Controlled Substances in 1971 in the Psychotropic Substances section [6]. However, the recreational use of magic mushrooms has continued to this day, although there have been periods when prevalence has been lower.

During the last decade, obtaining magic mushrooms has become easier, with sales in smart shops or over the Internet, through various

* Corresponding author at: Universidad de Alcalá, Departamento de Ciencias de la Computación, Ctra. Madrid-Barcelona km 33.6, Alcalá de Henares, Madrid 28864, Spain (F.E. Ortega-Ojeda).
E-mail addresses: csmesteves@gmail.com (C.S.M. Esteves), fernando.ortega.uah@gmail.com (F.E. Ortega-Ojeda).

https://doi.org/10.1016/j.forc.2022.100421
Received 15 December 2021; Received in revised form 5 April 2022; Accepted 5 April 2022
Available online 8 April 2022

forms such as fresh, air-dried, encapsulated power, and home-growing kits. Thus, the use of hallucinogenic mushrooms has created a problem in Europe, with a rising trend [7,8]. They are especially attractive to young people, as it is a safe and natural drug, and thus there is less sense of guilt. In 2018, magic mushrooms were the 9th most consumed drug, among 37 different drugs studied [9]. In addition, some researchers believe that the components of magic mushrooms may have therapeutic potential, which stimulates their consumption [8,10]. Therefore, there is a need for methods to identify magic mushrooms or to quantify the psilocybin and psilocin.

Current techniques for the analysis of magic mushrooms can be based on morphological characteristics [4,11], DNA [12–14], immunoassay [12] or chemical composition, mainly by chromatographic techniques [15–21].

The identification based on morphological characteristics fails when two or more species are visually very similar but have different uses, *e.g.*, edible and poisonous species. There are more than 50,000 species of mushrooms in nature, so it is very likely to find at least two similar species. The DNA molecular techniques are time consuming and costly. The immunoassay methods such as the enzyme-linked immunosorbent assay (ELISA) are faster than the DNA-based methods, but they require testing of the specific antibodies [12].

Chromatographic methods allow a qualitative and quantitative identification of the psilocybin and psilocin. They are very useful in analysing the presence of psilocin in biological samples, including hair samples [22]. However, analysis of the compounds of magic mushrooms requires sample preparation, namely extraction of the compounds, which may increase the time between harvest and analysis [22–24]. Also, the average content of hallucinogenic compounds is usually not higher than 2%, which requires advanced techniques [11,21,25,26].

The alternatives to chromatographic techniques are spectroscopic techniques, which are simple and often non-destructive. They can be used on a wide range of samples, including complex ones such as fungi. Some studies using IR on the mycological field [27–32] included magic mushrooms [33,34], some of which were performed with the extracted compounds to obtain simpler spectra. Nonetheless, the analysis of the mushrooms as they occur, *i.e.*, without any extraction process, could be of great interest. This is possible, but the obtained spectra are hardly interpretable. A mushroom spectrum is a set of vibrational bands of proteins, lipids and polysaccharides, at least with many IR active molecular vibrations [35,36]. To interpret this type of spectra, statistical tools are usually needed, such as chemometric analysis.

IR combined with multivariate analysis has been successfully used to analyse mushrooms and food samples [37–40]. Besides, there is considerable interest in using these two techniques: IR spectroscopic techniques, such as Attenuated Total Reflectance (ATR), which do not require extensive sample preparation, since the samples can be analysed fresh or dried, and the spectra acquisition is rapid. Then, chemometrics allows the interpretation of a large number of spectra simultaneously, the construction of a model, and the use of this model for prediction.

In particular, several studies reported the suitability of this techniques in forensic fields, mainly to combat fraud and counterfeiting of mushrooms with high commercial value. Wang et al., used raw and second derived FTIR-ATR spectra to discriminate between Lingzhi species, which are medicinal mushrooms. They applied partial least squares discriminant analysis (PLS-DA) classification models [41]. Li et al., developed a new FTIR and UV–Vis analytical approach to distinguish Ganodermataceae mushrooms, which also have therapeutic applications. They found that the model could discriminate species among varieties of marketing mushrooms and detect adulterations of Ganodermataceae [42]. Baeva et al., [43] combined FT -MIR, FT -NIR, and Raman to characterize *Pleurotus ostreatus*, and the chemometric models could be used to predict the macromolecular components. Segelke et al., [44] studied edible truffles, which are considered the most expensive fungi and are highly susceptible to adulteration. Truffle species could be distinguished using FT -NIR and PCA.

Edible and medicinal mushrooms have been studied, but to date no study has investigated the identification of magic mushrooms using spectroscopic techniques and chemometrics based on the fruiting bodies. Only psilocin has been analysed using IR [45].

Therefore, the aim of this work was to analyse edible, toxic and hallucinogenic mushrooms using FTIR-ATR without any sample preparation and then to find similarities and discrepancies on the IR spectra using chemometrics. In particular, an OPLS-DA method was used to discriminate magic mushrooms. In this study, a database of different mushrooms categories was implemented to identify a blind mushroom sample in order to provide a simple, non-destructive and sufficiently inexpensive alternative for rapid identification of hallucinogenic mushrooms.

2. Materials and methods

The wild mushrooms samples were collected in nature, in the regions of Alcalá de Henares (Madrid, Spain), and Guadalajara (Castilla La Mancha, Spain). The commercial samples were bought in a local supermarket or cultivated in the Department of Life Sciences of University of Alcalá, Alcalá de Henares (Spain). One of the "magic truffle sclerotium sample" known as "*Psilocybe hollandia*", was bought from a Dutch website. Both standards: Psilocybin (1.0 mg/mL in acetonitrile: water (1:1) P-097 Cerilliant) and psilocin (1.0 mg/mL in acetronitrile, P-098 (Cerilliant) were purchased from MilliporeSigma (aka Sigma Aldrich, Merck KGaA, St. Louis, MI, USA).

This work analysed 64 samples of 32 different mushrooms species. The species and the respective category are reported in the next section.

All samples were analysed after being dried under specific stable conditions. The abundant mushroom samples were sliced into small and fine pieces, which were put on a mesh, protected from the sun light, and dried for two weeks with very soft ventilation. The samples were dried at room temperatures in the 20 °C to 30 °C range, along the Spanish dry summer (Fig. 1). All dried samples were stored in closed (hard yet flexible polypropylene) conical tubes at 2 °C until their analysis. This method was recommended by the group's botanical experts in order to avoid damages in the tissue's composition.

The spectral collection was performed with a mid-IR spectrometer Thermo Scientific Attenuated Total Reflectance Fourier Transform Infrared (FTIR-ATR) Nicolet iS10, equipped with a Smart Diamond ATR accessory, a DTGS detector, and a KBr beam-splitter (Thermo Scientific, Waltham, MA, USA). Each spectrum was recorded in the 4000 cm^{-1} to 650 cm^{-1} range, with a resolution of 4 cm^{-1}, and 32 or 64 scans. The analysis of each mushroom species was performed on areas corresponding to the stalk, gills and cap (unless some of these tissues were not available). One spectrum was collected from two different points of the same piece, with other five replicates from other (different) mushroom pieces. The spectra sampling was done this way because there were plenty of dried samples, hence, the mushroom spectra could indeed guarantee variability even after being averaged. For the actual spectra

Fig. 1. Drying procedure for a hallucinogenic species Psilocybe cubensis var. amazonian.

collection, all samples were pressed against the crystal by means of the ATR's built-in presser, which ensured that the samples were always in constant contact with the crystal. The IR spectra of the psilocybin and psilocin standards were collected by putting a drop of the standard solution above the ATR crystal and letting the solvent evaporate at room temperature. A spectral pre-processing (baseline correction with baseline offset, Standard Normal Variate (SNV), and Savitzky-Galay method (second polynomial order, 7 points each side) preceded the statistical analysis with Orthogonal Partial Least Squares-Discriminant Analysis (OPLS-DA) using SIMCA software (Sartorius Stedium Biotech, Göttingen, Germany). The data pre-processing is imperative to ensure that the data is standardized and entirely comparable. The pre-processing sequence was always performed verifying that neither the data nor the results were degraded, *i.e.*, negatively affected. The software fitted automatically the OPLS-DA model, with as many components (predictive, orthogonal in X and orthogonal in Y) as considered significant. The autofit algorithm used seven cross-validation groups.

3. Results and discussion

3.1. Mushrooms identification

The samples' identification was performed according to their morphological characteristics.

Table 1 shows a summary of the mushroom species used in this work, as well as their category and origin. For some species, more than 1 sample, *i.e.*, mushrooms obtained at different locations or different times, was analysed, as shown in the table.

Table 1
Mushroom's species and their respective category, used as samples in this study. E – edible; T – toxic; H – hallucinogenic; NI – no interest/ no information. The Psilocybe varieties were not included yet in the Index Fungorum database. Nevertheless, they were discriminated in this work.

Species	Category	Origin	Number of samples
Agaricus bisporus	E	Supermarket, fresh	3
Agaricus iodosmus	T	Nature, fresh	1
Agaricus urinascens	E	Nature, dried	3
Cyclocybe (=*Agrocybe*) *cylindracea*	E	Nature, fresh	2
Amanita muscaria	T	Nature, fresh	2
Amanita phalloides	T	Nature, fresh	2
Saproamanita (=*Amanita*) *vittadinii*	E	Nature, dried	1
Calocybe gambosa	E	Nature, dried	1
Coprinopsis (=*Coprinus*) *atramentaria*	T	Nature, fresh	1
Cortinarius purpurascens	E	Nature, fresh	1
Geopora sumneriana	NI	Nature, dried	1
Hebeloma sinapizans	T	Nature, fresh	1
Hygrophorus marzuolus	E	Nature, dried	2
Lactarius vinosus	E	Nature, fresh	2
Lepista nuda	E	Nature, fresh	3
Lepista personata	E	Nature, dried	2
Lepiota subincarnata	T	Nature, fresh	2
Leucopaxillus gentianeus	NI	Nature, fresh	1
Lyophyllum loricatum	E	Nature, fresh	2
Picoa juniperi	T	Nature, dried	1
Pleurotus eryngii	E	Nature, fresh	2
Pleurotus eryngii var. *ferulae*	E	Cultivated, dried	1
Pleurotus ostreatus	E	Supermarket, fresh	2
Psathyrella candolleana	NI	Nature, dried	1
Psilocybe cubensis var. amazonian	H	Cultivated, fresh	12
Psilocybe cubensis var. colombiana	H	Cultivated, fresh	2
Psilocybe hollandia sclerotium	H	Internet, dried	2
Psilocybe semilanceata	H	Nature, dried	1
Russula xerampelina	E	Nature, fresh	3
Sarcosphaera coronaria	T	Nature, dried	1
Sparassis crispa	E	Nature, fresh	1
Tricholoma saponaceum	T	Nature, fresh	2

3.2. Spectral analysis

The FTIR-ATR spectra collection and analysis was performed in the standards (psilocybin and psilocin) and different mushrooms species.

3.2.1. Standards

For understanding if psilocybin and/or psilocin can have some contribution on the mushroom's spectra, their respective IR spectra were analysed, and their bands were assigned (Fig. 2). The detection of the spectra wavenumbers was performed within the OMNIC software (Thermo Fisher, Version 8.3, USA).

Psilocybin and psilocin structures are very similar, only differing in the 4-position group. For this reason, both spectra have characteristic vibrations of the indole ring and the amine group.

In the psilocin spectrum, a sharp medium intense band was easily visualized at 3396 cm^{-1}, which can correspond to the N–H stretching ν_{N-H}, from the 5-membered ring. The same feature appeared in psilocybin as an intense broad band between nearly 3700 and 3200 cm^{-1}. The multiple bands observed between 3100 and 2750 cm^{-1}, in psilocin and psilocybin, are a combination of all the C–H stretching vibrations. In psilocybin, this band is broader.

In the 1650–650 cm^{-1} region, some intense and sharp bands were visualized, which are mostly related with the C–H bending vibration δ_{C-H} and also with the rings vibrations.

The bands at around 1630–1615, 1600–1575, and 1520–1470 cm^{-1}, can be associated to the ring vibrations [46]. Due to the noise, these bands are not so well visualized in the psilocybin spectrum. Also, the bands between 1290 and 990 cm^{-1} correspond to the in-phase carbon stretching vibrations of the ring [47].

The C–H deformation vibrations appear nearly between 1465 and 1350 cm^{-1}. At higher frequencies, there are the out-of-phase (aka, asymmetric) deformation, and at lower wavenumber, the band represents the symmetric bending vibration [46]. The high number of bands between about 990 and 700 cm^{-1} are related to the C–H wagging vibration.

Regarding the 4-group position, psilocin has a hydroxyl substituent in this position, which gives rise to a broad band at around 3340–3120 cm^{-1}, which is related to the O–H stretching vibration. On the contrary, psilocybin has the bands corresponding to the phosphate group. First,

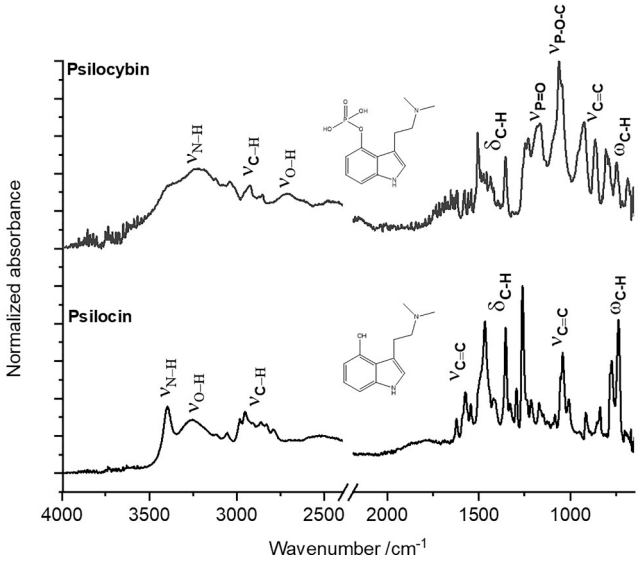

Fig. 2. IR spectra of psilocybin (above) and psilocin (below).

the O–H stretching vibration from the P-OH group, which appears in the 2800–2100 cm^{-1} range as a broad band at a lower frequency than the other O–H groups. The P=O stretching vibration appears at 1160 cm^{-1} while the P-O-C stretching vibration appears at 1060 cm^{-1}.

3.2.2. *Mushrooms species*

Mushrooms, in general, are expected to have different chemical composition in the different tissues [30]. This fact was verified in this study, with caps, gills and stalks showing different IR spectra (See Supplementary material). While the caps and stalks spectra had more similarities, the gills spectra seemed to be more distinctive. In magic mushrooms, the hallucinogenic compounds are expected to be in higher content in the cap and gills than in stalks [11].

Mushrooms have some nutrients like lipids, carbohydrates and proteins, which are highly variable, depending on the species.

Three mushroom species were used in this work: hallucinogenic (*Psilocybe cubensis* var. *amazonian*), toxic (*Tricholoma saponaceum*), and edible (*Pleurotus eryngii*) (Fig. 3). This work focused on the tissues with more expected hallucinogenic compounds, *i.e.*, the gills and then caps. The gills in particular offer and extra advantage over the caps since gills are more distinctive among species. The results are comparable among the different categories of the species.

The analysis of the three species' spectra revealed that they all present a broad medium-intensity band in the 3400–3000 cm^{-1} range. Considering that the samples were completely dried, these bands should be mostly due to the carbohydrates O–H stretching vibrations. The broad band shape was very similar in almost all spectra and, for this reason, the region between 4000 and approximately 3000 cm^{-1}, was not included into the chemometrics analysis, reported in next section.

The edible and toxic species have very similar spectra (Fig. 3). *Pleurotus eryngii*, *Tricholoma saponaceum* and also other species, show a weak band at 3010 cm^{-1}, which can be attributed to the = C–H stretching from the fatty acids unsaturated carbons or aromatic structures, related to the mushrooms pigments [30]. Because of the constant force of the sp or sp2 hybridized carbons, the = CH or –CH groups stretching vibrations are always detected above 3000 cm^{-1}. Interestingly, the hallucinogenic species, which have aromatic structures belonging to psilocybin and/or psilocin, do not show this band in their spectra. This corroborates the fact that their content on hallucinogenic compounds is not high enough to be detected by the naked eye in their spectra.

In the 2970–2830 cm^{-1} range, the occurrence of bands is reported to belong to the aliphatic C–H, corresponding to the respective stretching vibrations. There is a large discrepancy regarding these bands intensities between the hallucinogenic sample and the other two samples. In *Pleurotus eryngii* and *Tricholoma saponaceum* there are two very intense sharp bands. The same does not occur in *Psilocybe cubensis* var. *amazonian*.

Then, in the 1800 and 900 cm^{-1} region, the *Psilocybe cubensis* spectrum also has more number and intensities of different bands.

In *Psilocybe cubensis*, the band at 1633 cm^{-1} corresponds to the Amide I vibration, which means the proteins C = O stretching [30,48]. Usually, the carboxylic acids or esters C = O stretching vibration is located at a higher wavenumber, which may indicate the lower fats contribution on this specie. The Amide II vibration appears soon after, at 1539 cm^{-1}. The C-H out-of-phase bending vibration was reported to

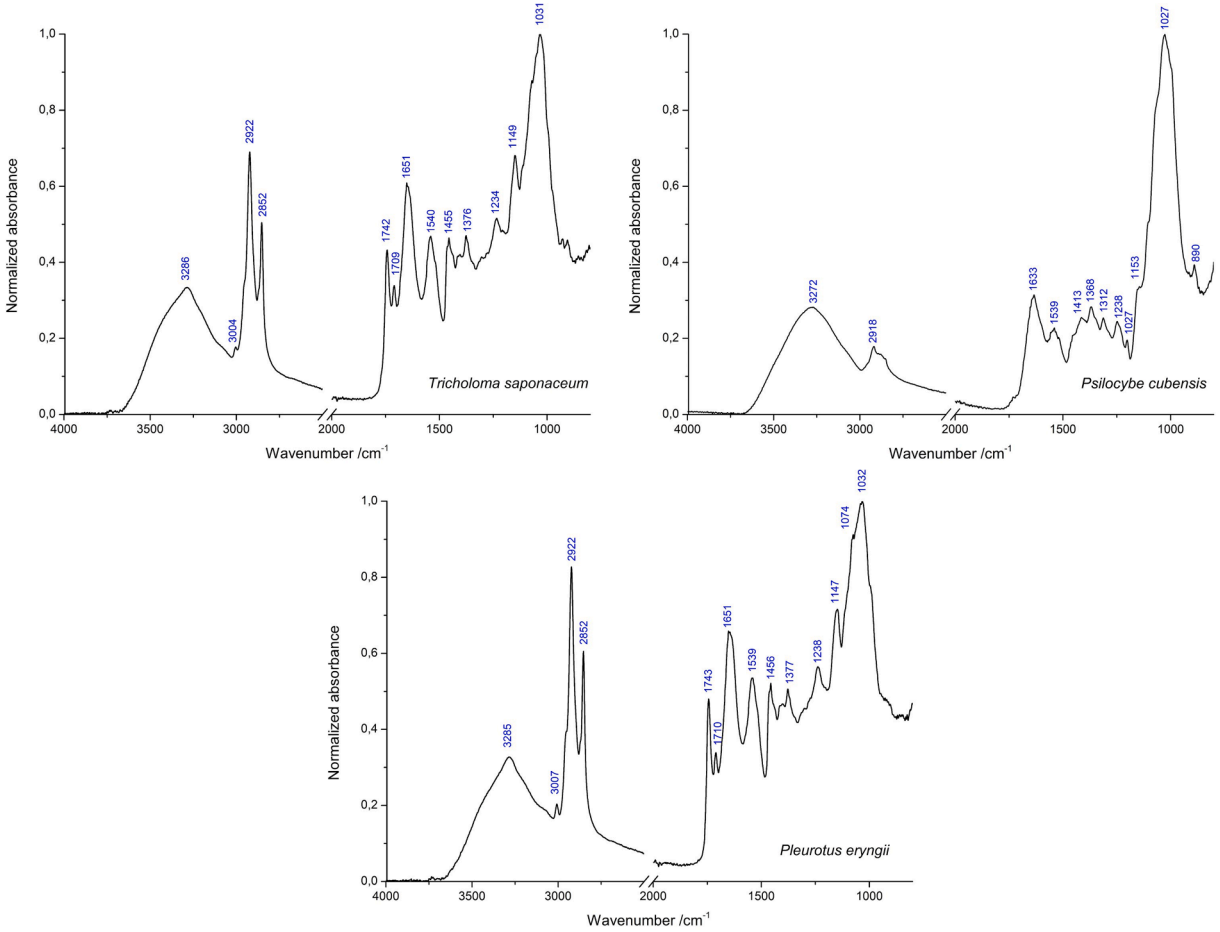

Fig. 3. IR spectra of the three mushroom species used in this work: hallucinogenic (Psilocybe cubensis var. amazonian), toxic (Tricholoma saponaceum), and edible (Pleurotus eryngii).

appearing at the 1413 cm^{-1} frequency, as well as the C-O-H bending. However, the in-phase bending of the C–H was reported at 1368 cm^{-1} [40,47]. The bands at 1248 and 1201 cm^{-1} are related to the pyranose ring C–C stretching vibration, and also with the carboxylic acids or esters C-O stretching [30]. The glycosidic linkage C-O-C stretching vibration appears at lower frequencies; at around 1153 cm^{-1} [32,37].

Then, the strong and broad band at around 1027 cm^{-1}, would be related to the alcohols C-O stretching, mainly from the polysaccharides. Some contribution from the C–C stretching vibrations may also arise. If there is a band related to the P-O-C stretching, from psilocybin or even from lipids, it could be hidden in this region. The weak band at 890 cm^{-1} can be related to the polysaccharides with β-linkages; it can be from the polysaccharides or glycosidic bonds C–H deformation [30,32].

In opposition to *P. cubensis*, both *T. saponaceum* and *P. eryngii* had signals at nearly 1743 and 1710 cm^{-1}. The first, according to literature, is attributed to the C = O stretching vibration of the carbonyl group in carboxylic acids or esters. The second, with lower intensity but also sharp, can be related to the protonated acid [30]. The next bands, with wavenumbers at 1651 and 1539 cm^{-1}, approximately, can also be associated to the Amide I and Amide II vibrations, respectively. As mentioned before, the bands at 1456 and 1401 cm^{-1} could arise due to the C-H out-of-phase vibration and C-O-H bending, and the band at 1377 cm^{-1} would appear due to the in-phase bending of the C-H. The C-C stretching vibration should be the responsible for the band at 1238 cm^{-1}. The band at 1147 cm^{-1}, as well as the bands with maximums at 1074 and 1032 cm^{-1}, could be due to the tertiary alcohols from the polysaccharides. However, this high intensity band can also be associated to the C-C stretching vibrations. In *P. eryngii*, two bands were detected between 1080 and 1030 cm^{-1}, while in *T. saponaceum* just one appeared. Besides, in the last spectrum, a little shoulder could be seen at the left of 1031 cm^{-1}, which could be related to the polysaccharides C-H deformation.

Usually, the combination of the C=O stretching vibrations which are not from the Amide I, with the CO vibrations and the C-H, are indicative of the lipids presence and can be used to detect them [37]. In these three analysed species, the largest differences seem to be in the lipids content, where the hallucinogenic species may have less lipids content than the edible or toxic species. Table 2 summarizes all the vibrations with the respective wavenumber and assignation.

The conclusions derived from the IR analysis would be transferable to the different species of mushrooms. Below is the chemometric analysis of the different parts of all the analysed mushrooms.

Table 2
Wavenumbers where there is a band on the IR spectra of the respective mushroom species, with the assignment.

Pleurotus eryngii	*Psilocybe cubensis*	*Tricholoma saponaceum*	Assignment
3285	3272	3286	O-H stretching
3007		3004	C-H stretching in aromatic structures
2922	2918	2922	C-H asymmetric stretching
2852		2852	C-H symmetric stretching
1743		1742	C = O stretching from lipids
1710		1709	
1651	1633	1651	Amide I
1539	1537	1540	Amide II
1456	1413	1455	C-H out-of-phase deformation
1401		1404	from CH_2/CH_3
1377	1368	1376	C-H in-phase bending
	1312		
1238	1248	1234	C-C stretching in pyranose ring
	1201		C-O stretching from acids and esters
1147	1153	1149	C-O-C stretching of glycosidic bond
1074			C-O stretching from alcohol
1032	1027	1031	groups (polysaccharides)
			C-C stretching
	890		C-H deformation of polysaccharides

3.3. Chemometric analysis

The chemometric analysis of gills, caps and stalks, was performed separately, as they have different chemical composition [30]. The OPLS-DA method was optimized for gills, and then adapted for both caps and stalks. Although several centring and scaling methods were tested prior the full validation procedure (results not shown), the spectral data was finally scaled using the Pareto without centring (ParN) method since it gave the best results. The software was set to calculate the boundaries with 95 % probability to counterweigh for any magnitude unbalance and/or variance that may exist [49]. This helped eliminating any weight because of the variables or observations magnitude. The analysis was done using a non-linear iterative partial least squares (NIPALS) algorithm, fully cross validation (CV) with uncertainty test, and 1/SDev as weighing. Because OPLS-DA is sensitive to the model complexity [49], and to avoid overfitting, the repeated 7-fold CV was set to estimate the relevant number of components in the OPLS models. Nonetheless, in order to stay on the safe side of the model fitting, less than five latent variables were use in all cases.

The method selection was followed by the analysis of the scores and loadings plots, for each tissue.

3.3.1. Gills

The gills OPLS-DA model was obtained from the 580 spectra. Scores scatter plot of the OPLS-DA model for the dried gills indicates the samples position, which allows visualizing some groups, depending on the sample's classes (Fig. 4). The 7-fold (groups) CV autofit algorithm suggested five predictive t[1–5] and 22 orthogonal to [1–22] variables. However, as can be seen, the separation of the Hallucinogenic class was already clear using only the one t[1] and two t[2] predictive variables. The R^2X[1] parameter indicated that about 8.9 % of the X (spectra) variation was modelled by the predictive t[1] component. Likewise, R^2X[2] showed that 5.2 % of the X variation was modelled by the predictive t[2] component. Moreover, the two orthogonal to[1–2] components modelled 76.6 % of the X variation. In other words, the joined R2 from only t[1–2] + to[1–2] explained about 90.7 % of the X (spectra) separation of the 580 samples.

The scores plot shows that most of the hallucinogenic species (yellow points) tended to stay near the plot origin, on the positive side of the 1st OPLS-DA component. All the hallucinogenic samples *Psilocybe cubensis* var. amazonian, *Psilocybe cubensis* var. colombiana, and *Psilocybe semilanceata* were closer to each other. A species/category identification can be obtained if the scores representing the mushrooms species are well defined in the space and distant from other species.

Loadings scatter plot of the OPLS-DA model is useful for understanding the relationship between the samples and the original variables (Fig. 5).

In this figure, the higher the contribution of the original variable to the component, the farther from the origin are the loadings. Hence, the variables with higher weights for the 1st OPLS-DA component are in the shaded areas coloured either in blue (for positive values) or in red (for negative values). IR spectrum of the dried gills is shown (Fig. 6) indicating the blue and red coloured variables with higher weights in loadings plot of the OPLS-DA model for dried gills (Fig. 5).

Almost all the bands of the IR spectrum are in the negative side of the 1st OPLS-DA component. The positive loadings in the 1st OPLS-DA component have larger contribution to the scores located on the same side. On the contrary, the negative loadings are related to the scores located on the negative axis for the same component (basically edible and toxic mushrooms). Those loadings showed larger dispersion (variations), which would indicate that the major mushrooms' constituents govern most of the toxic and edible species.

Conversely, the loadings that would correspond to the

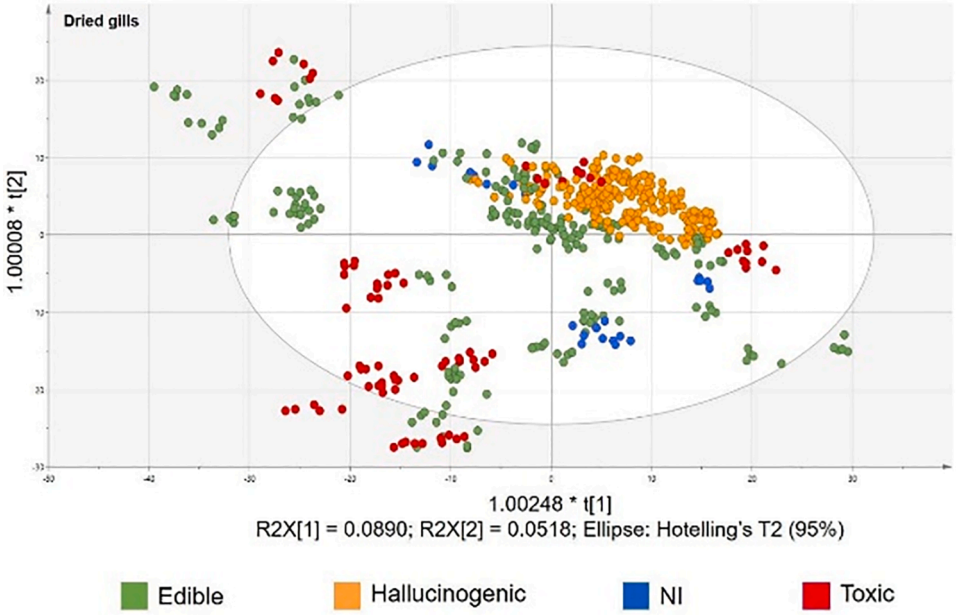

Fig. 4. Scores scatter plot of the OPLS-DA model for the dried gills.

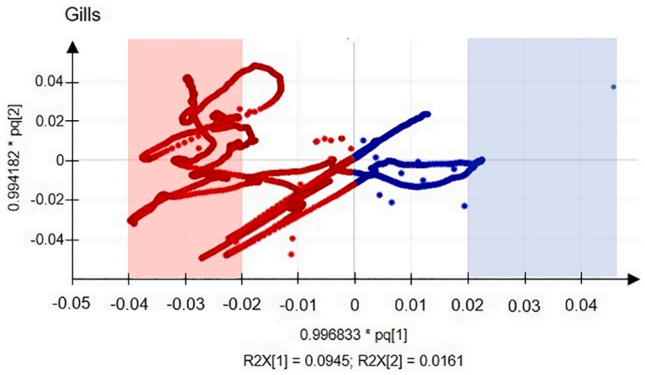

Fig. 5. Loadings plot of the OPLS-DA model for dried gills.

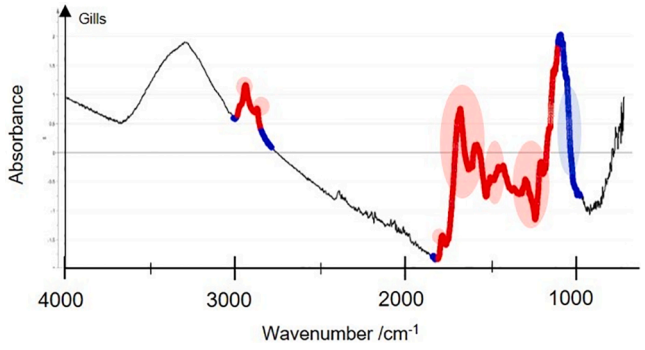

Fig. 6. IR spectrum of the dried gills, showing the bands corresponding to the loadings positions in the positive side of the 1st PLS component (blue) and in the negative side (red).

hallucinogenic mushrooms (the blue wavenumbers) did not vary much and had a strong relationship with the band at nearly 1040 cm^{-1}. This region does not represent a maximum of a visible band, which would imply that there is a hidden band in that region. However, performing the second derivative of the spectrum did not improve the results.

The phosphate group of psilocybin, as seen before, has a band from the P-O-C stretching vibration, which may appear in this region. Therefore, even the specific psilocybin bands cannot be detected in the IR spectrum, which could have some influence on its discrimination.

Besides, all hallucinogenic species were all together in a certain region of the scores plot that is rather close to some of the toxic and edible species. In order to increase the discrimination power, a new OPLS-DA model was calculated with the species located in the centre. The Scores scatter plot for this new model (Fig. 7) shows a clear discrimination of the hallucinogenic species (shaded areas) compared to the other species. The 7-fold (groups) CV autofit algorithm suggested five predictive t[1–5] and 21 orthogonal to[1–21] variables. However, the separation of the Hallucinogenic class was clear using only the three t[1–3] predictive and three to[1–3] orthogonal components. The $R^2X[1]$ parameter indicated that about 4.6 % of the X (spectra) variation was modelled by the predictive t[1] component. Similarly, $R^2X[2]$ showed that 1.3 % of the X variation was modelled by the predictive t[2] component. Also, $R^2X[3]$ indicated that about 1 % of the X variation was modelled by the predictive t[3] component. Moreover, the three orthogonal to[1–3] components modelled 88.3 % of the X variation. That is, the joined R^2 from only t[1–3] + to[1–3] explained about 94.7 % of the X (spectra) separation of the 406 samples.

3.3.2. Caps

In the Scores scatter plot of the OPLS-DA model performed on the dried caps (Fig. 8), samples are coloured by their category, where the yellow groups represent the hallucinogenic species. The 7-fold (groups) CV autofit algorithm suggested five predictive t[1–5] and 23 orthogonal to[1–23] components. However, the separation of the Hallucinogenic class was rather clear using only the two t[1–2] predictive and two to[1–2] orthogonal components. The $R^2X[1]$ parameter indicated that about 9.3 % of the X (spectra) variation was modelled by the predictive t[1] component, whilst $R^2X[2]$ showed that 1.2 % of the X variation was modelled by the predictive t[2] component. In addition, the two orthogonal to[1–2] components modelled 83.4 % of the X variation. That is, the joined R^2 from only t[1–2] + to[1–2] explained about 93.9 % of the X (spectra) separation of the 503 samples. Similar to the dried gills, the model for the caps resulted in a very good explanation and even better prediction in X-variables. However, the hallucinogenic species were more dispersed in the scores plot.

The *Psilocybe semilanceata* samples (the yellow scores at the bottom

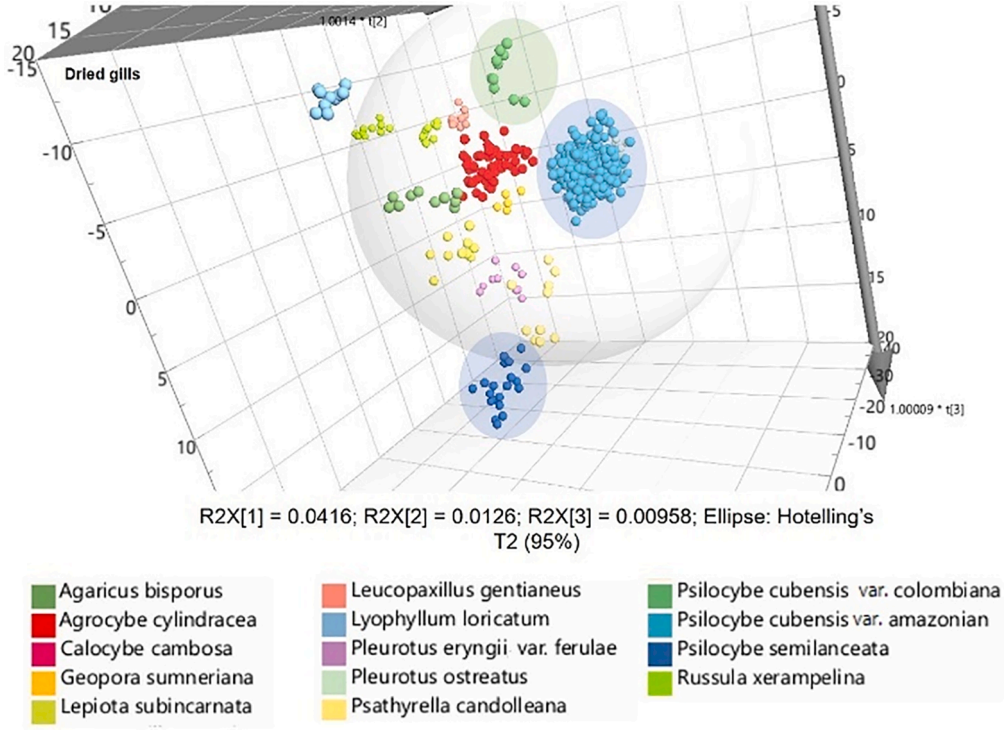

Fig. 7. Scores scatter plot of the reduced OPLS-DA model performed on the dried gills, coloured by their category.

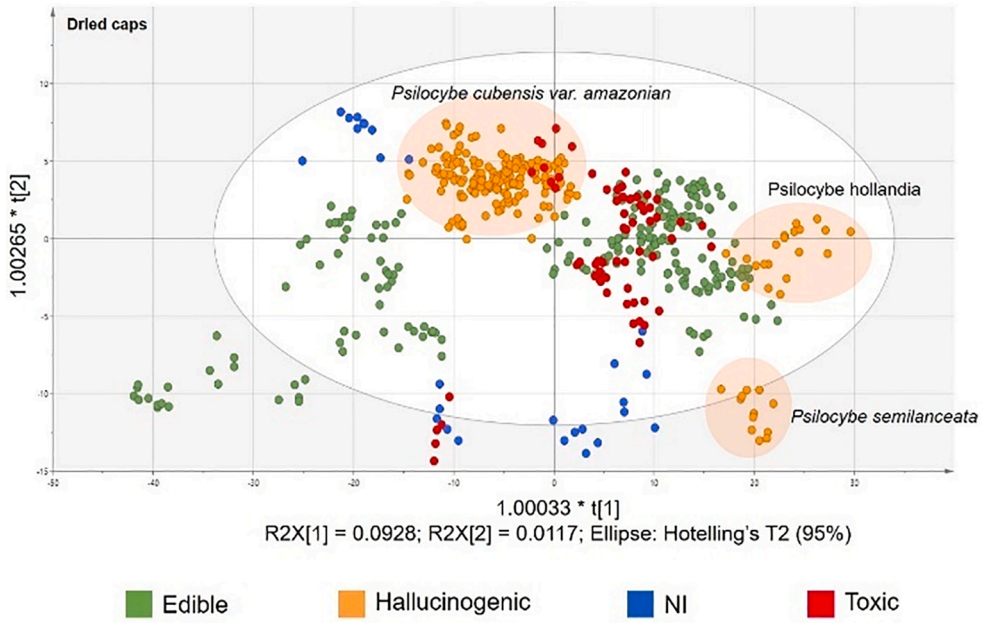

Fig. 8. Scores scatter plot of the OPLS-DA model performed on the dried caps coloured by their category. The yellow regions represent the hallucinogenic species with the respective name.

of Fig. 8) were well separated from the other samples, that is, they can be easily identified in this samples' library. *Psilocybe hollandia* (the yellow scores just above *Psilocybe semilanceata*) was closer to *Psilocybe semilanceata* than to *Psilocybe cubensis* var. amazonian. This could mean that this magic truffle is chemically more similar to *Psilocybe semilanceata*.

For loadings scatter plot of the OPLS-DA model for the dried caps (Fig. 9), the variables with higher weights for the 1st OPLS-DA component, are located in the shaded areas coloured either in blue (for positive values) or in red (for negative values).

Loadings of the 1st PLS component and the position of the positive (blue) and the negative (red) sides (Fig. 9) are represented in IR spectrum of a dried cap (Fig. 10). *Psilocybe cubensis* var. amazonian had a different contribution comparing to the behaviour of the gills. That is, the position near the origin of the 1st OPLS-DA component, in the negative side, correlated to the loadings coloured in red. This difference can be understood as a consequence of different chemical composition between gills and caps. *Psilocybe semilanceata*, on other side, is in a similar position comparing to the gills.

Scores scatter plot was calculated with the central samples after excluding the already discriminated samples (Fig. 11). The 7-fold

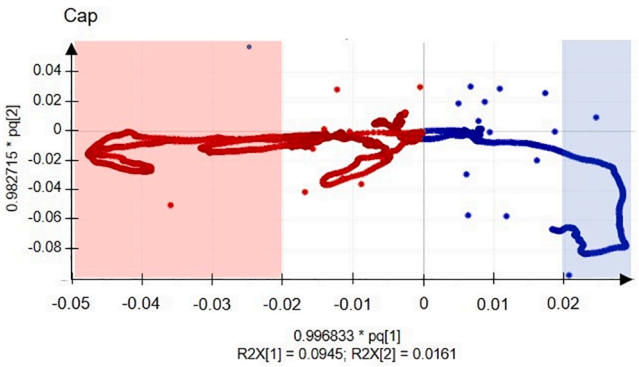

Fig. 9. Loadings scatter plot of the OPLS-DA model for the dried caps.

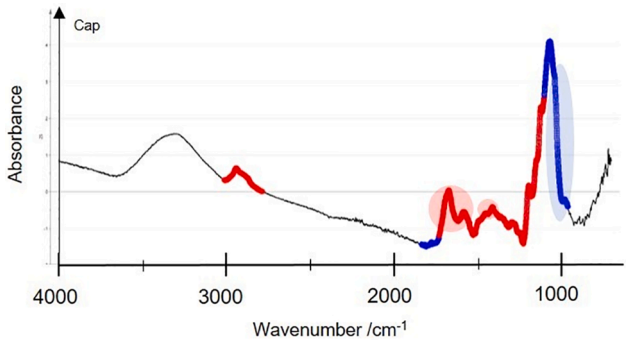

Fig. 10. IR spectrum of a dried cap, representing the Loadings of the 1st PLS component. It shows the position of the positive (blue) and the negative (red) sides from Fig. 9.

(groups) CV autofit algorithm suggested five predictive t[1–5] and 23 orthogonal to[1–23] components. However, the separation of the *Psilocybe cubensis* var. amazonian class was clear using only the two t[1–2] predictive and two to[1–2] orthogonal components. The $R^2X[1]$ parameter indicated that about 4.7 % of the X (spectra) variation was modelled by the predictive t[1] component, while $R^2X[2]$ showed that 0.7 % of the X variation was modelled by the predictive t[2] component. In addition, the two orthogonal to[1–2] components modelled 88.7 % of the X variation. These results mean that, the joined R2 from only t[1–2] + to[1–2] explained about 94.0 % of the X (spectra) separation of the 394 samples. Rotating the 3D representation allowed visualizing all the discriminated samples, including *Psilocybe hollandia*.

3.3.3. Stalks

There were 446 available samples of dried mushrooms stalks. Their slightly lower number compared to gills or caps, was because not all the species had the three distinguishable parts. Scores scatter plot of the OPLS-DA model was performed on the dried stalks samples (Fig. 12). Although a model reduction was also performed like in the last two cases, no model improvements were achieved. The 7-fold (groups) CV autofit algorithm suggested five predictive t[1–5] and 23 orthogonal to [1–23] components. However, the separation of the Hallucinogenic class was acceptable using only the two t[1–2] predictive and two to[1–2] orthogonal components. The $R^2X[1]$ parameter indicated that about 8.5 % of the X (spectra) variation was modelled by the predictive t[1] component, whilst $R^2X[2]$ showed that 1.2 % of the X variation was modelled by the predictive t[2] component. Moreover, the two orthogonal to[1–2] components modelled 84.0 % of the X variation. These results mean that, the joined R^2 from only t[1–2] + to[1–2] explained about 93.7 % of the X (spectra) separation of the 446 samples. Although the hallucinogenic species were more dispersed in this graph and it was harder to see well-defined groups, the fitting values were a little bit better than those for gills, but worse than those for caps.

Loadings scatter plot of the OPLS-DA model for the dried stalks (Fig. 13) indicates that their behaviour was more similar to caps than to gills. IR spectrum of a dried stalk (Fig. 14) shows the variables which contribute more to the Loadings of the 1st PLS component. With these graphs, we confirmed that the chemical composition of caps and stalks is quite similar. As the score of the hallucinogenic species in the caps and stalks are in the negative side of the 1st OPLS-DA component, the blue-coloured bands contribution was not so high as in gills. This may be

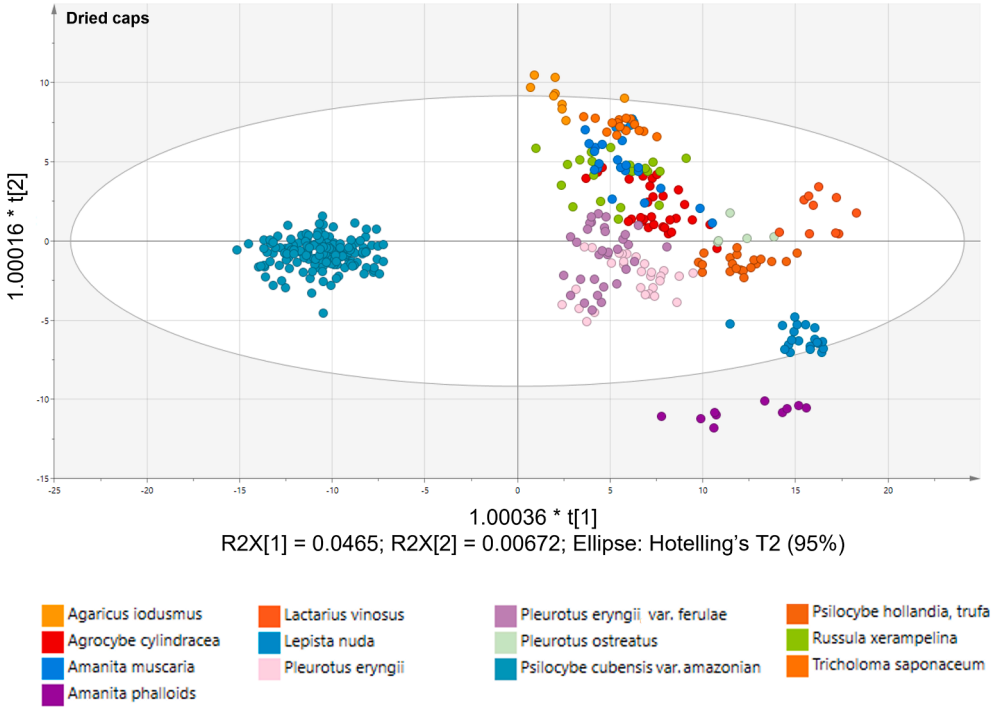

Fig. 11. Scores scatter plot of the reduced OPLS-DA model performed on the dried caps samples, coloured by their category.

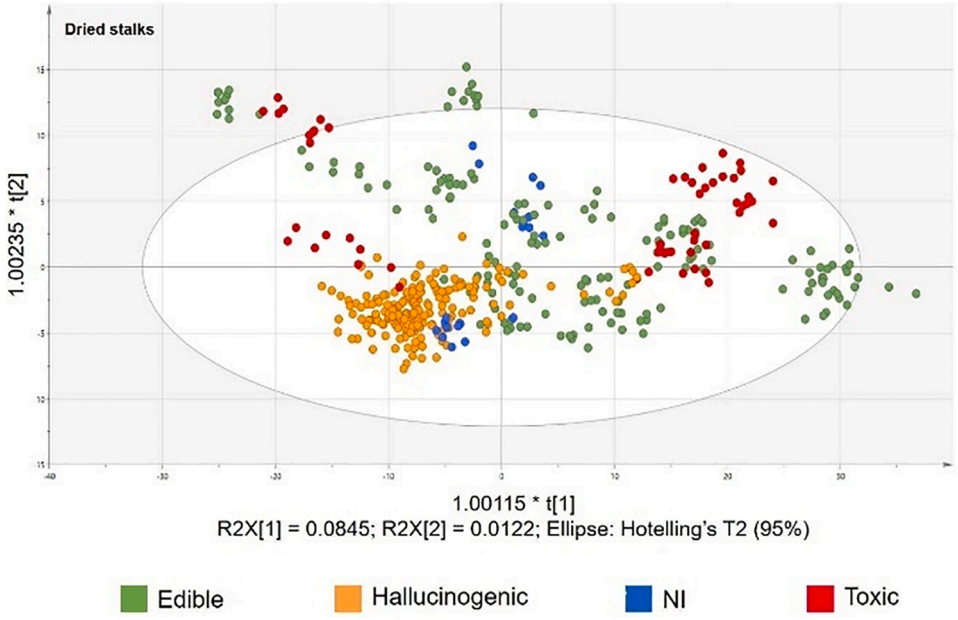

Fig. 12. Scores scatter plot of the OPLS-DA model performed on the dried stalks samples, coloured by their category.

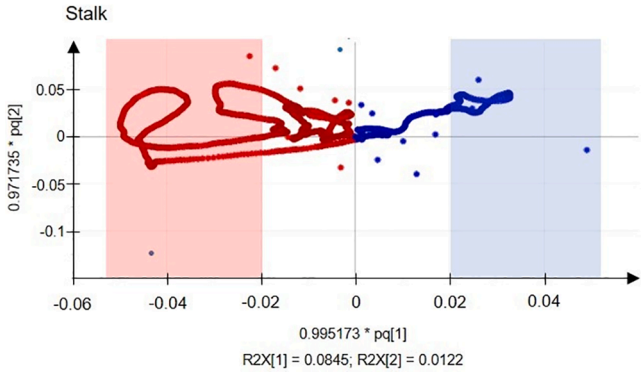

Fig. 13. Loadings scatter plot of the OPLS-DA model for the dried stalks.

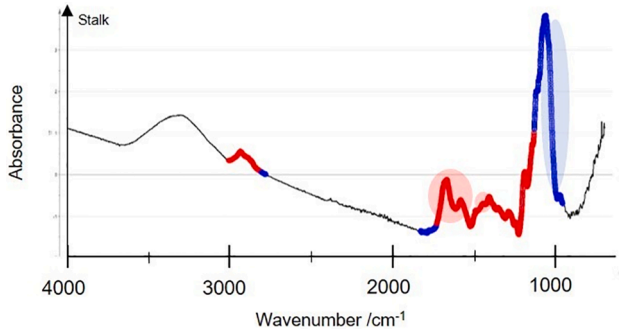

Fig. 14. IR spectrum of a dried stalk, representing the loadings of the 1st PLS component. It shows the position of the positive (blue) and the negative (red) sides in Fig. 13.

related to the previous results about the psilocybin/psilocin quantification: The content of hallucinogenic compounds is higher in gills than in any other tissue [11].

Other interesting results should be pointed out: some of the toxic species are well discriminated in all the presented scores plots. These outcomes can be helpful in accidental intoxication cases, where, sometimes, people get poisoned because of eating mushrooms. *Amanita phalloides* is a deadly species, which can easily be mistake with edible mushrooms. A quick identification of the consumed mushroom may provide a more efficient medical treatment, thus saving a person's life.

4. Conclusions

The proliferation of magic mushrooms in online media, as the safest drug in the world, poses a problem for the safety of people, users and non-users, leading to the illegal consumption of magic mushrooms. The identification of mushrooms generally requires the knowledge of an experienced mycologist. Due to the still low prevalence of magic mushroom consumption, it is not common for forensic laboratories to have mycologists. Therefore, the identification of toxic mushrooms becomes difficult when a sample is seized. In addition, current chemical methods for direct identification of psilocybin or psilocin are destructive and time consuming.

This work used a rapid, simple, and solvent-free method to distinguish magic mushrooms without the need to prepare samples prior to analysis. The method combined both FTIR-ATR and chemometrics.

The analysed mushroom samples consisted of various dried tissues from different fruiting bodies of several mushrooms species. There are reports indicating differences in the IR spectra of gills, caps and stalks, which would confirm that the chemical composition of mushrooms varies depending on the piece [30]. In the case of the gill spectra, the vibrational bands could only be assigned to the major constituents of the mushrooms, which are clearly visible in the spectra. In other words, the vibrational bands of non-abundant components, specifically from psilocybin or psilocin were not visible to the naked eye. Therefore, OPLS-DA regression models were developed on the mushrooms IR spectra for each dried piece. That is, the models used an IR spectral collection containing different mushrooms species [34]. When using dried mushrooms, the best models resulted from analysing the gills and caps. Both results showed that the magic mushrooms tended to stay in only one quadrant of the graphical representation. Fitting a new model with only the magic mushrooms along with the surrounding samples allowed for the complete discrimination of the hallucinogenic, edible, and toxic species. This can be used for species identification, or at least to know which category the mushrooms belong to. In the case of the stalks, the magic mushrooms could not be well distinguished, but the poisonous

species could.

In addition, this study included the "magic truffles", which are a new alternative to the traditional fresh or dried hallucinogenic mushrooms. Their discrimination was achieved from the dried cap spectra collection. Truffles do not belong to the fruiting bodies of mushrooms: they are sclerotia. For this reason, many countries have not yet included them in their national laws, so they are legal consumption products. Nevertheless, the use of OPLS-DA regression modelling allowed the identification of *Psilocybe hollandia* in the studied collection.

The results obtained in this work can be very useful in forensic laboratories because nowadays the IR technique and devices are very common in modern laboratories. This is because the technique is easy to use, non-destructive and fast, requiring almost no sample preparation, and the mushroom's spectral library could be shared among the forensic experts for their practical casework use. Moreover, the use of multivariate analysis allowed the discrimination of hallucinogenic or toxic species, in a large data set. Even a non-expert can perform this methodology in the field. This work has enabled the discrimination of hallucinogenic mushrooms inside a collection of edible and toxic species. The additional discrimination of toxic species is an important advantage that can be applied in clinical cases of fungi poisoning.

CRediT authorship contribution statement

Cátia S.M. Esteves: Methodology, Investigation, Formal analysis, Writing – original draft, Writing – review & editing. **Elena M.M. de Redrojo:** Methodology, Investigation, Formal analysis, Writing – original draft, Writing – review & editing. **José Luis García Manjón:** Conceptualization, Resources, Writing – review & editing. **Gabriel Moreno:** Conceptualization, Resources, Writing – review & editing. **Filipe E. Antunes:** Supervision, Writing – review & editing. **Gemma Montalvo García:** Conceptualization, Investigation, Resources, Supervision, Writing – review & editing. **Fernando E. Ortega-Ojeda:** Conceptualization, Formal analysis, Software, Resources, Writing – review & editing.

Declaration of Competing Interest

The authors declare that they have no known competing financial interests or personal relationships that could have appeared to influence the work reported in this paper.

Acknowledgements

Cátia Esteves would like to thank Erasmus + programme of the European Union for her "Learning Agreement for Traineeships" and the CINQUIFOR investigation group for the assistance and technical support. Authors also thank to Félix Zapata for the help in the experimental work.

Appendix A. Supplementary data

Supplementary data to this article can be found online at https://doi.org/10.1016/j.forc.2022.100421.

References

[1] O. Shirota, W. Hakamata, Y. Goda, Concise large-scale synthesis of psilocin and psilocybin, principal hallucinogenic constituents of "magic mushroom", J. Nat. Prod. 66 (6) (2003) 885–887.
[2] K. Stebelska, Chapter 84 - Assays for Detection of Fungal Hallucinogens Such as Psilocybin and Psilocin, in: Neuropathology of Drug Addictions and Substance Misuse, Academic Press, San Diego (2016), pp. 909–926.
[3] L.-Y. Feng, A. Battulga, E. Han, H. Chung, J.-H. Li, New psychoactive substances of natural origin: a brief review, J. Food Drug Anal. 25 (3) (2017) 461–471.
[4] G. Moreno, J.L. Manjón **Guía de hongos de la Península Ibérica**, Omega(2010).
[5] C. Andersson, J. Kristinsson, J. Gry, Occurrence and use of hallucinogenic mushrooms containing psilocybin alkaloids, Nordic Concil of Ministers, Copenhagen, Denmark (2009).
[6] United Nations Office on Drugs Crime, Final act of the United Nations Conference for the adoption of a protocol on psychotropic substances, in: The International Drug Control Conventions, United Nations(2013).
[7] T. Mishraki-Berkowitz, E. Kochelski, P. Kavanagh, J. O'Brien, C. Dunne, B. Talbot, P. Ennis, U.E. Wolf The Psilocin (4-hydroxy-N,N-dimethyltryptamine) and Bufotenine (5-hydroxy-N,N-dimethyltryptamine) Case: Ensuring the Correct Isomer has Been Identified Journal of Forensic Sciences, 65(5) (2020), pp.1450-1457.
[8] J. Solano, L. Anabalon, S. Figueroa, C. Lizama, L.C. Reyes, D. Gangitano, Psychedelic fungus (Psilocybe sp.) authentication in a case of illegal drug traffic: sporological, molecular analysis and identification of the psychoactive substance, Sci. Justice 59 (1) (2019) 102–108.
[9] A.R. Winstock, M.J. Barratt, A. Aldridge, A. Zhuparris, E. Davies, C. Hughes, M. Johnson, M. Kowalski, J.A. Ferris, Global Drug Survey (GDS) Key Findings Report, 2019.
[10] M. Farré, E. Papaseit, F. Fonseca, M. Torrens, Addiction of Hallucinogens, Dissociatives, Designer Drugs and "Legal Highs": Update on Potential Therapeutic Use, in: Textbook of Addiction Treatment: International Perspectives, Springer International Publishing, Cham (2021), pp. 259-279.
[11] K. Tsujikawa, T. Kanamori, Y. Iwata, Y. Ohmae, R. Sugita, H. Inoue, T. Kishi, Morphological and chemical analysis of magic mushrooms in Japan, Forensic Sci. Int. 138 (1) (2003) 85–90.
[12] I. Morita, H. Oyama, Y. Kiguchi, A. Oguri, N. Fujimoto, A. Takeuchi, R. Tanaka, J. Ogata, R. Kikura-Hanajiri, N. Kobayashi Immunochemical monitoring of psilocybin and psilocin to identify hallucinogenic mushrooms Journal of Pharmaceutical and Biomedical Analysis, 190 (2020), p.113485.
[13] B. Kallifatidis, J. Borovička, J. Stránská, J. Drábek, D.K. Mills, Fluorescent Random Amplified Microsatellites (F-RAMS) analysis of mushrooms as a forensic investigative tool, Forensic Sci. Int. Genet. 9 (2014) 25–32.
[14] V. Gambaro, G. Roda, G.L. Visconti, S. Arnoldi, E. Casagni, L. Dell'Acqua, F. Farè, E. Paladino, C. Rusconi, S. Arioli, D. Mora, DNA-based taxonomic identification of basidiospores in hallucinogenic mushrooms cultivated in "grow-kits" seized by the police: LC-UV quali-quantitative determination of psilocybin and psilocin, J. Pharm. Biomed. Anal. 125 (2016) 427–432.
[15] T. Kamata, M. Nishikawa, M. Katagi, H. Tsuchihashi, Liquid chromatography-mass spectrometric and liquid chromatography-tandem mass spectrometric determination of hallucinogenic indoles psilocin and psilocybin in "Magic Mushroom" Samples, J. Forensic Sci. 50 (2005) 336–340.
[16] R. Kikura-Hanajiri, M. Hayashi, K. Saisho, Y. Goda, Simultaneous determination of nineteen hallucinogenic tryptamines/β-calbolines and phenethylamines using gas chromatography–mass spectrometry and liquid chromatography–electrospray ionisation-mass spectrometry, J. Chromatogr. B 825 (1) (2005) 29–37.
[17] T. Keller, A. Keller, E. Tutsch-Bauer, F. Monticelli, Application of ion mobility spectrometry in cases of forensic interest, Forensic Sci. Int. 161 (2) (2006) 130–140.
[18] J. Borovička, M. Oborník, J. Stříbrný, M.E. Noordeloos, L.A. Parra Sánchez, M. Gryndler, Phylogenetic and chemical studies in the potential psychotropic species complex of Psilocybe atrobrunnea with taxonomic and nomenclatural notes, Persoonia 34 (2014) 1–9.
[19] K. Saito, T. Toyooka, M. Kato, T. Fukushima, O. Shirota, Y. Goda, Determination of psilocybin in hallucinogenic mushrooms by reversed-phase liquid chromatography with fluorescence detection, Talanta 66 (3) (2005) 562–568.
[20] J.R. Stenzel, W.S. Patrol, G. Jiang, C. Loran, Identification of Psychotropic Substances in Mushrooms and Chocolate by UHPLC/MS, Thermo Fisher Scientific Inc, 2008. [21] J. Nagy, T. Veress.
[21] J. Nagy, T. Veress, HPLC analysis of hallucinogenic mushroom alkaloids (Psilocin and Psilocybin) applying hydrophilic interaction chromatography (HILIC), J. Forensic Res. 07 (06) (2016).
[22] L. Zhou, P. Xiang, D.i. Wen, B. Shen, X. Wang, L.e. Li, H. Deng, H. Chen, H. Yan, M. Shen, Y. Shi, W. Liu, Sensitive quantitative analysis of psilocin and psilocybin in hair samples from suspected users and their distribution in seized hallucinogenic mushrooms, Forensic Toxicol. 39 (2) (2021) 464–473.
[23] N. Rácz, J. Nagy, W. Jiang, T. Veress, Modeling retention behavior on analysis of hallucinogenic mushrooms using hydrophilic interaction liquid chromatography, J. Chromatogr. Sci. 57 (3) (2019) 230–237.
[24] T. Veress, N. Rácz, J. Nagy, W. Jiang Determination of Psilocin and Psilocybin in Magic Mushrooms Using iHILIC ® -Fusion and MS LC GC Europe, 2019 (2019).
[25] N. Anastos, S.W. Lewis, N.W. Barnett, D.N. Sims, The determination of psilocin and psilocybin in hallucinogenic mushrooms by HPLC utilizing a dual reagent acidic potassium permanganate and tris(2,2'-bipyridyl)ruthenium(II) chemiluminescence detection system, J. Forensic Sci. 51 (1) (2006) 45–51.
[26] R. Kysilka, M. Wurst, A novel extraction procedure for psilocybin and psilocin determination in mushroom samples, Planta Medica 45 (3) (1990) 327–328.
[27] Y. Chen, B. Chefetz, R. Rosario, J.D.H. van Heemst, C.P. Romaine, P.G. Hatcher Chemical Nature and Composition of Compost During Mushroom Growth Compost Science & Utilization, 8(4) (2000), pp.347-359.
[28] Y.K. Choong, J. Lan, H.L. Lee, X.-D. Chen, X.-G. Wang, Y.-P. Yang, Differential identification of mushrooms sclerotia by IR macro-fingerprint method, Spectrochim. Acta Part A Mol. Biomol. Spectrosc. 152 (2016) 34–42.
[29] A.J. Michell, G. Scurfield, Composition of extracted fungal cell walls as indicated by infrared spectroscopy, Arch. Biochem. Biophys. 120 (3) (1967) 628–637.

[30] V. Mohaček-Grošev, R. Božac, G.J. Puppels, Vibrational spectroscopic characterization of wild growing mushrooms and toadstools, Spectrochim. Acta Part A Mol. Biomol. Spectrosc. 57 (14) (2001) 2815–2829.
[31] Y. Ma, H. He, J. Wu, C. Wang, K. Chao, Q. Huang, Assessment of polysaccharides from mycelia of genus ganoderma by mid-infrared and near-infrared spectroscopy, Sci. Rep. 8 (1) (2018) 1–10.
[32] A. Synytsya, K. Míčková, A. Synytsya, I. Jablonský, J. Spěváček, V. Erban, E. Kováříková, J. Čopíková, Glucans from fruit bodies of cultivated mushrooms Pleurotus ostreatus and Pleurotus eryngii: structure and potential prebiotic activity, Carbohydr. Polym. 76 (4) (2009) 548–556.
[33] A.Y. Leung, A.G. Paul, Baeocystin and norbaeocystin: new analogs of psilocybin from psilocybe baeocystis, J. Pharm. Sci. 57 (10) (1968) 1667–1671.
[34] A. Koçak, L.M.D. Cotiis, D.B. Hoffman, Comparative study of ATR and transflection IR spectroscopic techniques for the analysis of hallucinogenic mushrooms, Forensic Sci. Int. 195 (1) (2010) 36–41.
[35] P. Kalač, Chemical composition and nutritional value of European species of wild growing mushrooms: a review, Food Chem. 113 (1) (2009) 9–16.
[36] G.K. Gomba, A. Synytsya, P. Švecová, M.A. Coimbra, J. Čopíková, Distinction of fungal polysaccharides by N/C ratio and mid infrared spectroscopy, Int. J. Biol. Macromol. 80 (2015) 271–281.
[37] A.A. Kulmyrzaev, R. Karoui, J.D. Baerdemaeker, E. Dufour, Infrared and fluorescence spectroscopic techniques for the determination of nutritional constituents in foods, Int. J. Food Prop. 10 (2) (2007) 299–320.
[38] A. O'Gorman, G. Downey, A.A. Gowen, C. Barry-Ryan, J.M. Frias, Use of fourier transform infrared spectroscopy and chemometric data analysis to evaluate damage and age in mushrooms (Agaricus bisporus) grown in Ireland, J. Agric. Food. Chem. 58 (13) (2010) 7770–7776.
[39] A. Hirri, M. Bassbasi, S. Platikanov, R. Tauler, A. Oussama, FTIR spectroscopy and PLS-DA classification and prediction of four commercial grade virgin olive oils from morocco, Food Anal. Methods 9 (4) (2016) 974–981.
[40] S. Yao, T. Li, J. Li, H. Liu, Y. Wang, Geographic identification of Boletus mushrooms by data fusion of FT-IR and UV spectroscopies combined with multivariate statistical analysis, Spectrochim. Acta Part A Mol. Biomol. Spectrosc. 198 (2018) 257–263.
[41] Y.Y. Wang, J.Q. Li, H.G. Liu, Y.Z. Wang, Attenuated total reflection-fourier transform infrared spectroscopy (ATR-FTIR) combined with chemometrics methods for the classification of lingzhi species, Molecules 24 (12) (2019).
[42] X.-P. Li, J. Li, H. Liu, Y.-Z. Wang, A new analytical method for discrimination of species in Ganodermataceae mushrooms, Int. J. Food Prop. 23 (1) (2020) 227–240.
[43] E. Baeva, R. Bleha, M. Sedliaková, L. Sushytskyi, I. Švec, J. Čopíková, I. Jablonsky, P. Klouček, A. Synytsya, Evaluation of the cultivated mushroom pleurotus ostreatus basidiocarps using vibration spectroscopy and chemometrics, Appl. Sci. 10 (22) (2020) 8156.
[44] T. Segelke, S. Schelm, C. Ahlers, M. Fischer Food Authentication: Truffle (Tuber spp.) Species Differentiation by FT-NIR and Chemometrics Foods, 9(7) (2020).
[45] M. Meenu, B. Xu, Application of vibrational spectroscopy for classification, authentication and quality analysis of mushroom: a concise review, Food Chem. 289 (2019) 545–557.
[46] G. Socrates Infrared and Raman Characteristic Group Frequencies, Wiley-Blackwell (2004).
[47] P. Larkin, Infrared and Raman Spectroscopy: Principles and Spectral Interpretation, (2nd Ed)., Elsevier, 2018.
[48] A. Barth, C. Zscherp, What vibrations tell about proteins, Q. Rev. Biophys. 35 (4) (2002) 369–430.
[49] M. Bylesjö, M. Rantalainen, O. Cloarec, J.K. Nicholson, E. Holmes, J. Trygg, OPLS discriminant analysis: combining the strengths of PLS-DA and SIMCA classification, J. Chemom. 20 (8) (2006) 341–351.